Diffusion length of positrons and positronium investigated using a positron beam with longitudinal geometry

S. Van Petegem,[1,2] C. Dauwe,[1,*] T. Van Hoecke,[1] J. De Baerdemaeker,[1] and D. Segers[1]
[1]*Department of Subatomic and Radiation Physics, Ghent University, Proeftuinstraat 86, B-9000 Gent, Belgium*
[2]*NUM/ASQ, Paul Scherrer Institute, CH-5232, Villigen, Switzerland*
(Received 8 March 2004; revised manuscript received 12 May 2004; published 14 September 2004)

Positronium emission from single crystalline Al_2O_3, MgO and vitreous a-SiO_2 surfaces was studied as a function of the positron implantation energy E by means of Doppler broadening spectroscopy and Compton-to-peak ratio analysis. When the Ge-detector is in-line with the positron beam, the emission of para-positronium yields a red-shifted fly-away peak with intensity I^{e}_{pPs}. An analysis of I^{e}_{pPs} versus E for Al_2O_3 and MgO where no Ps is formed in the bulk ($f_{\mathrm{Ps}}=0$) results in positron diffusion lengths $L_{+}(Al_2O_3)=(18\pm1)$ nm and $L_{+}(\mathrm{MgO})=(14\pm1)$ nm, and efficiencies for the emission of Ps by picking up of a surface electron of $f_{pu}(Al_2O_3)=(0.28\pm0.2)$ and $f_{pu}(\mathrm{MgO})=(0.24\pm0.2)$. For a-SiO_2 the bulk Ps fraction is $f_{\mathrm{Ps}}(a\text{-}SiO_2)=(0.72\pm0.01)$, $f_{pu}(a\text{-}SiO_2)=(0.12\pm0.01)$ and the diffusion lengths of positrons, para-positronium and ortho-positronium are $L_{+}(SiO_2)=(8\pm2)$nm, $L_{\mathrm{pPs}}(SiO_2)=(14.5\pm2)$ nm and $L_{\mathrm{oPs}}(SiO_2)=(11\pm2)=$nm. Depending on the specimen-detector geometry the emission of Ps at low implantation energy may cause either an increase or a decrease of the width of the annihilation line shape at low implantation energies.

DOI: 10.1103/PhysRevB.70.115410 PACS number(s): 78.70.Bj, 36.10.Dr

It is well-known that many solids emit positronium (Ps) when they are bombarded by slow positrons. This phenomenon is particularly interesting in wide band gap insulators such as some metal oxides, in porous low-k dielectrics and in the vast majority of polymeric materials. The literature abounds with reports on experiments where the Doppler broadened line shape parameter $S(E)$ is investigated in function of the energy of the implanted positrons, by means of a VEP—Variable Enery Positron beam. This method presents two not well documented problems. First, the value of the S parameter at the surface, i.e., at extrapolated zero implantation energy, may be either higher or lower than its corresponding value deep into the material. We will show that this effect is due to the particular geometry of the VEP. Second, when analyzing the evolution of S versus the implantation energy, one can obtain a diffusion length L. However the analysis of $S(E)$ data is unable to tell whether the diffusing particle is a positron or a positronium, and is unable to separate them if both are present. We will show that, with the proper geometry, and performing a detailed analysis of the annihilation line shape, one can obtain the diffusion lengths of positrons, para-positronium (pPs) and ortho-positronium (oPs). There are several mechanisms at the basis of Ps emission in insulators (for an overview see Ref. 1). The following processes to form Ps at the surface have been reported in the literature: (a) implanted positrons can diffuse to the surface, capture an electron and leave as Ps,[2] (b) implanted positrons can get trapped into a surface state that can be thermally activated into Ps emission,[3] and (c) Ps can be formed in the bulk of the material and can diffuse back to the surface where it is emitted.[4–6]

Time-Of-Flight (TOF) spectroscopy is the most accurate method to measure the energy distribution of emitted ortho-positronium (oPs) in a direct way. Sferlazzo[3,6] used this method to study oPs emission from Al, MgO and α-SiO_2 surfaces. Unfortunately the TOF technique needs a dedicated instrument to be built. As an alternative, Eldrup *et al.*[7] and later Rice-Evans and Smith[8] used Doppler broadening of annihilation radiation (DBAR) to study the emission of para-positronium (pPs), respectively, from ice crystals and a GaAs wafer surface at very low implantation energies. The 511 keV annihilation peak is broadened due to the conservation of energy and linear momentum of the annihilating positron-electron pair. A variable energy positron beam experiment (VEP) may be done with two different modes for the beam, sample and γ-ray detector. In the longitudinal mode the γ-ray detector is located behind the sample on the axis of the beam. For the transverse mode the line of sight of the γ-ray detector is perpendicular to the beam axis, i.e., parallel to the surface of the sample. In a longitudinal beam positronium emitted at the surface of a sample has a linear momentum mainly away from the detector. This linear momentum causes a red shift of the pPs contribution in the annihilation spectrum. In a transverse beam the fly-away pPs shows no red shift. In this paper we exploit the longitudinal mode to investigate the emission of Ps from single crystal Al_2O_3, MgO and vitreous a-SiO_2 surfaces. The a-SiO_2 specimen is particularly interesting because it is well known that it forms Ps in the bulk, and because its amorphous structure is a good analog to amorphous polymers, which may also benefit from this new approach.

The Doppler broadening measurements were performed in the longitudinal mode at the variable energy positron beam (VEP) in Ghent. The annihilation photons are detected by a high purity germanium (HPGe) detector with a full width at half maximum (FWHM) of 1.2 keV at 511 keV. The annihilation peaks were analyzed into three or four Gaussian distribution functions (see Fig. 1). Two main contributions have the same centroid, and they describe fairly well the low-momentum and the high-momentum contribution of the annihilations of positrons in the bulk and /or on the surface. The third Gaussian contribution is shifted toward

 ©2004 The American Physical Society

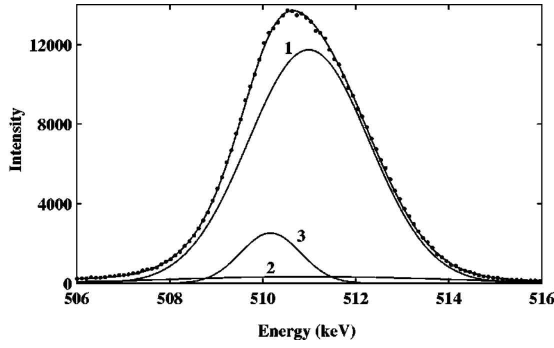

FIG. 1. Annihilation peak obtained from a MgO single crystal, fitted by a low momentum (1) and a high momentum (2) central Gaussian contribution and a red-shifted contribution (3) from the emitted pPs. The central pPs is absent in MgO and Al_2O_3. Due to its low intensity the background correction is not shown here.

low energy, and is due to the emitted pPs. A fourth contribution is also centered and has a narrow FWHM. This last contribution is identified as annihilation of pPs in the bulk. The Compton-to-peak ratio, as defined further in Eq. (7) and thereafter, is also observed as a probe for the emission of oPs. Two background corrections were used: a constant contribution due to the background level originating from external sources and a Compton background correction, based on the error-function.[9] As the positronium is emitted from the surface, the distance to the detector is increasing but due to its short lifetime, 99.9% of the emitted pPs annihilates within 1 mm from the surface. As a consequence the solid angle for detection of emitted pPs is the same as for positrons and Ps annihilating inside the material. When the detector is placed perpendicular to the normal of the sample no asymmetry in the annihilation peak was observed. Therefore one can assume that most of the pPs is emitted perpendicular to the surface. Consider a cylindrical detector with diameter $2R$ which is placed behind the specimen at distance d. In first approximation all annihilation photons which are emitted within the angle $\theta_{\max}=\arccos(d/\sqrt{R^2+d^2})$ are detected, where θ is the angle between the beam axis and the direction of emission of the radiation. The observed Doppler energy shift is $E_d=(c/2)p_z \cos\theta$, and its spatial mean value $\langle E_d\rangle$ is easily evaluated as

$$\langle E_d\rangle = \frac{cp_z}{4}(1+\cos\theta_{\max}), \tag{1}$$

where $p_z \cong p$ is the linear momentum of the emitted pPs.

The shape of the fly-away pPs peak $W(E_d)$ is a convolution of the Doppler shift distribution $w(p_z)$ with the intrinsic resolution function of the HPGe detector $g(\epsilon,\sigma)$:

$$W(E_d) \propto w(p_z) \otimes g(\epsilon,\sigma) \propto w(\sqrt{E_z}) \otimes g(\epsilon,\sigma), \tag{2}$$

where E_z is the longitudinal kinetic energy of the fly-away pPs, ϵ is the energy parameter for the convolution and σ is the Gaussian dispersion of the detector resolution function. As the detector resolution is roughly a Gaussian function, the pPs peak will be a Gaussian function only if its momentum distribution $w(\sqrt{E_z})$ is also a Gaussian function. TOF results on MgO and SiO_2 reported by Sferlazzo *et al.* show that the Ps energy distribution is an asymmetric function with a tail at the high energy side.[6] After transformation to momentum distributions, the experimental TOF curves are nearly symmetrical functions that deviate not more than 10% from a Gaussian function. Therefore it is justified to fit the fly-away pPs contribution with a Gaussian function. Because all the samples are insulators, charging effects have to be considered. At low implantation energies charging has a drastic influence on the count rate. Therefore in the analysis we only consider those measurements made with positrons with an energy of 200 eV and higher. Due to the high sensitivity of Ge-detectors to external influences such as temperature variations usually a digital stabilizer is used in Doppler broadening measurements. The stabilizer corrects the gain of the spectrum amplifier to balance the content of two regions chosen symmetrically around the 511 keV peak position. Due to the pPs contribution the annihilation peak is asymmetric and this asymmetry is changing as function of the implantation energy. As a consequence the stabilizer will correct the gain (and thus the calibration factor) as a function of the implantation energy and the correct energy information is affected. Therefore no stabilizer was used for our measurements. Usually positron diffusion lengths are calculated from the $S(E)$ curve using fitting routines such as VEPFIT.[10] In these routines it is assumed that each positron environment (surface, interface, layer1, layer2,…) has a characteristic value of the S-parameter. In the longitudinal mode the red shifted pPs causes a strong asymmetry of the peak and the S-parameter is no longer a simple linear combination of the characteristic values. Therefore we need a different approach. The positron implantation profile $P(z,E)$ of a monoenergetic beam with mean energy E is well approximated by the Makhov distribution:

$$P(z,E) = \frac{mz^{m-1}}{z_0^m}\exp[-(z/z_0)^m], \quad z_0 = \frac{\alpha}{\rho}\frac{E^n}{\Gamma\left(\frac{m+1}{m}\right)}, \tag{3}$$

with ρ the density of the material and m, n and α are, respectively, 2.0 ± 0.1, 1.62 ± 0.05 and 4.0 ± 0.3 μg cm^{-2} keV$^{-1.62}$, as reported by Vehanen *et al.*[11] If positronium is formed in the bulk material through the spur or the blob mechanism,[12–14] we may assume that the initial distribution of positronium is equal to the implantation profile of positrons. The fraction f_{Ps} of bulk positrons form Ps. The remaining fraction $(1-f_{Ps})$ of positrons can diffuse back to the surface and may emerge as oPs or pPs by picking up an electron from the surface. The fraction of the surface-positrons that capture such an electron is f_{pu}. The bulk Ps diffuses and is either trapped into free-volume sites of the amorphous structure, or reaches the surface whereupon it is ejected. The trapped oPs decays mainly through pick-off annihilation and the well known Eldrup formula describes the relation between its decay constant, $\lambda_{oPs} \cong \lambda_{po}$ and the radius of the trapping sites. The decay of trapped pPs is branched into pick-off annihilation and self annihilation, thus $\lambda_{pPs}=\eta\lambda_0^p+\lambda_{po}$, where η is the contact density of the Ps, $\lambda_0^p=1/124$ ps^{-1} is the decay constant of pPs in vacuum, λ_{pPs}

TABLE I. Results of positron lifetime measurements on Al_2O_3, MgO and a-SiO_2.

	τ_1 (ps)	τ_2 (ps)	τ_3 (ns)	I_1 (%)	I_2 (%)	I_3 (%)
Al_2O_3	80	160	–	20	80	–
MgO	–	195	–	–	100	–
SiO_2	150	550	1.6	23.6	16.9	59.5

and λ_{po} are obtained from a lifetime spectrum analysis (see Table I). Because of this branching only the fraction

$$f_b = \frac{\eta^{\lambda_0}}{\lambda_{pPs}} = \frac{\lambda_{pPs} - \lambda_{oPs}}{\lambda_{pPs}} \cong 0.906 \tag{4}$$

of pPs is observed as a "narrow" central contribution in Doppler or angular correlation measurements. The diffusion of any of these particles, and the fraction that reach the surface is given by[15,16]

$$F_j(E) = \int_0^\infty P(z,E)\exp(-z/L_j)dz, \tag{5}$$

where the subscript j stands for the positrons (+), and both states of positronium (pPs and oPs). The respective diffusion lengths are L_+, L_{pPs} and L_{oPs}. The following set of equations describe the intensities of fly-away para-positronium that is observed in the red-shifted contribution in the Doppler profile, the fly-away ortho-positronium that is observed in the Compton-to-peak ratio, and the fraction of bulk para-positronium that appears as a central narrow contribution in the Doppler profile:

$$I^{e}_{pPs} = (1/4)[fF_+(E) + f_s F_{pPs}(E)], \tag{6a}$$

$$I^{e}_{oPs} = (3/4)[fF_+(E) + f_s F_{oPs}(E)], \tag{6b}$$

$$I^{b}_{pPs} = (1/4)f_b f_{Ps}[1 - F_{pPs}(E)], \tag{6c}$$

where $f = f_{pu}(1 - f_{Ps})$. Equations (6) are greatly simplified for materials that do not form Ps in the bulk, such as Al_2O_3 and MgO, because then $f_{Ps}=0$, and it is sufficient to observe the fly-away pPs peak.

Figure 2 shows the intensity of the pPs flying away from the surface of single crystals of Al_2O_3 and MgO as function of the positron implantation energy. In the case of Al_2O_3 the intensity starts at 9% and decreases smoothly with increasing implantation energy until about 1500 eV whereas for MgO it starts at 8%. Above 1500 eV the intensity of the pPs peak is too low to be distinguished clearly from the central annihilation peak. From the fitting procedure we obtain the positron diffusion lengths $L_+ = 18 \pm 1$ nm for Al_2O_3 and $L_+ = 14 \pm 1$ nm for MgO. This value for Al_2O_3 coincides with the result obtained by Brauer *et al.*[17] for an α-Al_2O_3 specimen after annealing for 1 hour at 800 °C. Delocalized or Bloch Ps was never found in single crystal Al_2O_3 and MgO and we can assume that the Ps is formed at the surface by electron capturing.[18] The fitted values of these electron pick-up fractions are $f_{pu} = 0.28 \pm 0.02$ for Al_2O_3 and $f_{pu} = 0.24 \pm 0.02$ for MgO. Thus we see that of all positrons reaching the surface approximately 26% are emitted as Ps.

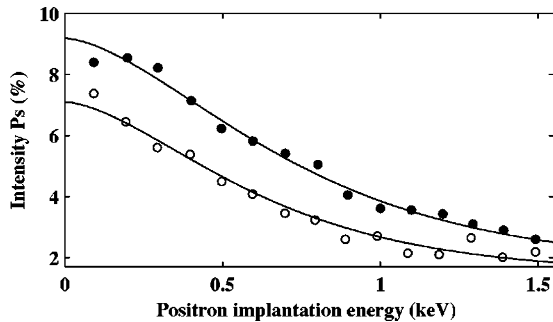

FIG. 2. Intensity the pPs peak emitted from an Al_2O_3 (•) and a MgO surface (◦) as function of the implantation energy. The solid lines represent the fit of Eq. (6a) to determine the diffusion length L_+.

Bulk positron lifetime measurements were performed to detect the existence of Ps in the bulk of the samples and to verify the trapping of the positrons in point defects such as vacancies. The results are shown in Table I. For Al_2O_3 and MgO no long oPs component is found. The single short lifetime that was found in MgO corresponds well to the value which was reported by Forster *et al.*,[19] who attributes it to saturation trapping in point defects. In the case of Al_2O_3 two short lifetimes were found. The longer one corresponds to the trapped state, and its intensity of 80% again indicates strong trapping.

In the case of vitreous a-SiO_2 three lifetime components were found, which are in agreement with values reported by Uedono *et al.*[20] The third lifetime of 1.6 ns is much longer than the maximum lifetime of positrons inside materials. This is an indication for the existence of oPs in the bulk of a-SiO_2. For delocalized Ps in single crystal α-SiO_2 a single lifetime of 283 ps was reported by Van Den Bosch *et al.*[21] We can conclude that the lifetime of 1.6 ns we find in the bulk of vitreous a-SiO_2 corresponds to the decay of oPs trapped inside free volumes of the amorphous structure. Thus the values to be used in Eq. (4) for SiO_2 are $\lambda_{pPs} = \tau_1^{-1}$ and $\lambda_{oPs} = \tau_3^{-1}$. The bulk pPs is also trapped in the free volume, and hence it mainly self-annihilates with isotropic low-momentum transfer. Therefore it is necessary to add the central narrow contribution to the analysis of the Doppler lineshape, and to observe the Compton-to peak ratio, in order to fully exploit the possibilities of Eqs. (6). The experimental fraction of emitted oPs is obtained from a Compton-to-peak ratio analysis of the annihilation spectrum at implantation energy E:

$$I^{\exp}_{oPs}(E) = \alpha\left[1 + \frac{P(0)}{P(\infty)}\frac{R(0) - R(E)}{R(E) - R(\infty)}\right]^{-1}, \tag{7}$$

where P is the number of counts in the peak area around 511 keV and $R = C/P$ is the ratio of the number of counts in a chosen fixed area of the Compton region C to the peak counts P. The values $P(\infty)$ and $R(\infty)$ are the asymptotic values for high implantation energy, i.e., in the bulk of the material, $P(0)$ and $R(0)$ are the values extrapolated to zero implantation energy. Equation (7) can only be applied if $P(\infty)$

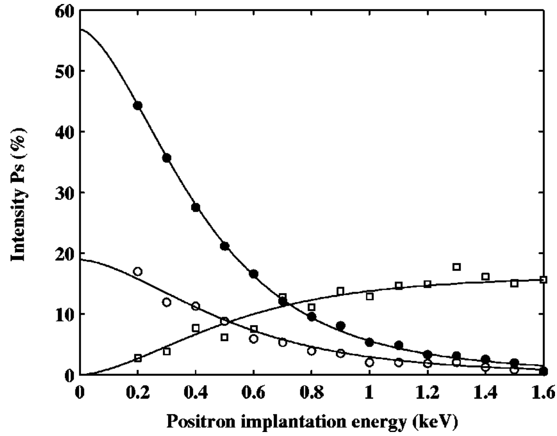

FIG. 3. Ps emission from a-SiO_2 as function of the implantation energy. The figure shows the intensity of the pPs emitted from the surface (∘), the intensity of pPs formed in the bulk (□) and the intensity of the emitted oPs (•). The solid lines represent the fit of Eq. (6) to determine the diffusion lengths L_+, L_{pPs} and L_{oPs}.

and $R(\infty)$ correspond to a situation where no oPs is detected by three-quantum annihilation. Of all positrons that are injected deep into the bulk $(E\rightarrow\infty)$ the fraction,

$$f_{3\gamma}(\infty) \cong I_3 \frac{\eta\lambda^0_{oPs}}{\eta\lambda^0_{oPs}+\lambda_{oPs}} \leqslant 0.0067, \qquad (8)$$

decays into three photons, where λ^0_{oPs} is the natural decay constant of oPs. Because $f_{3\gamma}(\infty)$ is at least 20 times smaller than $f_{3\gamma}(0)$, we may safely ignore this contribution. In contrast to pPs the fly-away oPs may annihilate several cm in front of the specimen, and thus the solid angle for the detection of the corresponding three-quantum annihilation is reduced by a factor ≈0.55 with respect to all two-quantum annihilation. This effect is taken into account by adjusting the value of the proportionality constant α in the following way: fitting of the first and second equation of (6) yields the zero-extrapolated values $I^e_{oPs}(0)$ and $I^e_{pPs}(0)$ and α is chosen so that $I^e_{oPs}(0)/I^e_{pPs}(0)=3$. For the linehape fittings of a-SiO_2 the $FWHM_E$ of the central pPs peak was fixed at a value which was estimated by 2 methods. Hasegawa *et al.*[22] determined the width in angular correlation of the bulk pPs in unirradiated a-SiO_2 as $FWHM_\theta=3.8$ mrad. From this we estimate $FWHM_E=(1/2)mc^2\ FWHM_\theta=0.97$ keV. On the other hand, using the Eldrup formula, the experimental lifetime of trapped oPs of 1.6 ns corresponds to a radius of the trapping center $R_0=4.12$ Å. According to Nakanishi,[23] $FWHM_\theta(\text{mrad})=16.6/R_0(\text{Å})$. From this we obtain $FWHM_E=4.24/R_0=1.02$ keV. The FWHM of the central pPs peak was therefore fixed to 1.6 keV, taking into account the intrinsic resolution of the HPGe detector at 511 keV. The experimental data for the intensities of the fly-away pPs, the fly-away oPs and the bulk pPs are shown in Fig. 3 together with the results from the fitting of Eq. (6). We see that the intensity of the central contribution (bulk pPs) increases as function of the positron implantation energy at the expense of the intensity of the red-shifted contribution (emitted pPs). The fitted diffusion lengths for a-SiO_2 are $L_+(SiO_2)=8\pm2$ nm, $L_{pPs}(SiO_2)=14.5\pm2$ nm and $L_{oPs}(SiO_2)=11\pm2$ nm. The diffusion lengths of ortho- and para-positronium are roughly equal. This is easily understood considering that $L=\sqrt{2nD/(\lambda+\kappa)}$ where λ is the decay constant of the free particle, κ is the trapping rate of the particle into some sink, n is the dimension of he diffusion process (i.e., $n=3$ in the case of bulk diffusion)[24] and D is the diffusion coefficient. For the bulk of a-SiO_2 all positronium is efficiently trapped into the free-volume sites, which means that $\kappa \gg \lambda$ both for oPs and pPs and thus $L_{oPs}\approx L_{pPs}\approx\sqrt{2nD_{Ps}/\kappa}$. Brauer *et al.*[25] reported a diffusion length of $L_+\sim21$ nm in a thick layer of thermally grown SiO_2, which was claimed to be identical to vitreous silica. These authors also remarked that the obtained L_+ values include both positrons and positronium. Our values for L_+, L_{pPs} and L_{oPs} are somewhat lower, most notably L_+. The reason might be that our experiments are performed at very low implantation energy $(0<E<1.6$ keV) and that epithermal positrons may reach the surface, in which case the diffusion is not in thermal equilibrium. This may enhance the emmision for very low energies, and thus shorten the apparent diffusion length L_+.

The fitting results in a total bulk Ps formation fraction $f_{Ps}=(0.73\pm0.05)$. This corresponds to an expected long lifetime intensity $I_3=(0.55\pm0.04)$ which agrees fairly well with the value of 0.595 which we obtained from the lifetime spectrum; see Table I. The fitted fraction of surface positrons that picks up an electron and is emitted as Ps is $f_{pu}=(0.12\pm0.01)$ which is approximately half as efficient as for Al_2O_3 and MgO.

These findings have implications for standard S versus E experiments. With longitudinal beam detector geometry the fly-away pPs increases the asymmetry of the peak and thus decreases the observed S-parameter for low implantation energy E. However,with a perpendicular beam-detector geometry the fly-away pPs is seen as a very narrow central contribution and the S parameter increases for low E. For materials that form Ps in the bulk and at the surface, such as SiO_2 and polymers, it is possible to obtain the three diffusion constants only if the intensities of bulk pPs, emitted pPs and emitted oPs are separately observed and the three equations (6) are solved simultaneously. Transverse VEP experiments yield only one mean S versus E relation. They are unable to distinguish the bulk pPs from the emitted pPs and are therefore not suitable to obtain the complete set of experimental parameters. Diffusion lengths obtained in the transverse mode are therefore to be treated with suspicion.

In our analysis we have approximated the lineshape $W(E_d)$ by a Gaussian distribution, and we do not expect to obtain a detailed description of the energy distribution of the emitted pPs. Therefore we plan to use coincidence Doppler broadening spectroscopy (CDB) in longitudinal geometry to study the emission of Ps. For this purpose the sample has to be rotated $\pi/4$ with respect to the beam axis, and the two detectors to be placed perpendicular to the sample surface. CDB has an improved peak-to-background ratio of a factor of 1000 and an improved effective energy resolution of a factor $\sqrt{2}$.

In conclusion, we have used Doppler broadening and red-shift spectroscopy and Compton-to-peak ratio to study posi-tronium emission for Al_2O_3, MgO and a-SiO_2 surfaces. We have shown for the first time that detailed analysis can yield the distinct diffusion lengths L_+, L_{pPs} and L_{oPs}, as well as the fraction f_{Ps} of positronium formed in the bulk and the fraction f_{pu} of positrons forming positronium at the surface by picking-up of an electron.

This research is part of the Interuniversity Poles of Attraction Program-(IUAP 5/1). It was furthermore supported by Fonds voor Wetenschappelijk Onderzoek—Vlaanderen (FWO).

*Corresponding author, Telephone: +32-9-264.65.68; fax: +32-9-264.66.97; electronic address: charles.dauwe@UGent.be

[1] C. Dauwe, T. Van Hoecke, and D. Segers, in *Condensed Matter Studies by Nuclear Methods*, Proceedings of XXX Zakopane School of Physics, edited by K. Tomala and E. Görlich (Institute of Physics, Jagiellonian University and H. Niewodniczański Institute of Nuclear Physics, Kraków, 1995), p. 275.

[2] R. Nieminen and J. Oliva, Phys. Rev. B **22**, 2226 (1980).

[3] P. Sferlazzo, S. Berko, and K. F. Canter, Phys. Rev. B **32**, 6067 (1985).

[4] M. Eldrup, A. Vehanen, P. J. Schultz, and K. G. Lynn, Phys. Rev. Lett. **51**, 2007 (1983).

[5] A. P. Mills and W. S. Crane, Phys. Rev. Lett. **53**, 2165 (1984).

[6] P. Sferlazzo, S. Berko, and K. F. Canter, Phys. Rev. B **35**, 5315 (1987).

[7] M. Eldrup, A. Vehanen, P. J. Schultz, and K. G. Lynn, Phys. Rev. B **32**, 7048 (1985).

[8] P. C. Rice-Evans and D. L. Smith, Phys. Lett. A **141**, 201 (1989).

[9] I. Chaglar, P. Rice-Evans, K. A. Marko, and A. Rich, Nucl. Instrum. Methods **187**, 581 (1981).

[10] A. van Veen, H. Schut, M. Clement, J. de Nies, A. Kruseman, and M. Ijpma, Appl. Surf. Sci. **85**, 216 (1995).

[11] A. Vehanen, K. Saarinen, P. Hautojärvi, and H. Huomo, Phys. Rev. B **35**, 4606 (1987).

[12] S. V. Stepanov and V. M. Byakov, *Principles and Applications of Positron and Positronium Chemistry* (World Scientific Singapore, 2003), pp. 117–146.

[13] C. Dauwe, B. Van Waeyenberge, and N. Balcaen, Phys. Rev. B **68**, 132202 (2003).

[14] C. Dauwe, B. Van Waeyenberge, and J. De Baerdemaeker, Mater. Sci. Forum **445–446**, 229 (2004).

[15] A. Dupasquier and A. Zecca, Riv. Nuovo Cimento **8**, 1 (1985).

[16] W. Swiatkowski, Nukleonika **48**, 141 (2003).

[17] G. Brauer, W. Anwand, E. M. Nicht, J. Kuriplach, I. Procházka, F. Bečvář, A. Osipowicz, and P. G. Coleman, Phys. Rev. B **62**, 5199 (2000).

[18] J. Major, A. Seeger, and O. Stritzke, Mater. Sci. Forum **105–110**, 1939 (1992).

[19] M. Forster, J. Mundy, and H. Schaefer, *Positron Annihilation* (World Scientific, Singapore, 1988), p. 833

[20] A. Uedono, T. Kawano, S. Tanigawa, and H. Itoh, J. Phys.: Condens. Matter **6**, 8669 (1994).

[21] A. Van Den Bosch, D. Segers, M. Tsumbu, L. Dorikens-Vanpraet, and M. Dorikens, Radiat. Eff. **74**, 161 (1983).

[22] M. Hasegawa, M. Saneyasu, M. Tabata, Z. Tang, Y. Nagai, T. Chiba, and Y. Ito, Nucl. Instrum. Methods Phys. Res. B **166–167**, 431 (2000).

[23] H. Nakanishi and Y. Jean, *Studies in Physical and Theoretical Chemistry 57: Positron and Positronium Chemistry* (Elsevier, Amsterdam, 1988), p. 176.

[24] J. Gebauer, F. Rudolf, A. Politi, R. Krause-Rehberg, J. Martin, and P. Becker, Appl. Phys. A: Mater. Sci. Process. **68**, 411 (1999).

[25] G. Brauer, W. Anwand, W. Skorupa, A. Revesz, and J. Kuriplach, Phys. Rev. B **66**, 195331 (2002).